

Low-cost weather sensor based on thermal impedance measurements

Heinrich Ruser, Michael Horn

Institute for Measurement and Automation,
University of Bundeswehr Muenchen, 85577 Neubiberg, Germany
heinrich.ruser@unibw.de

Abstract – Two examples of self-controlled wind and weather sensors for everyday usage based on temperature-dependent resistors are described and the potential for further enhancing sensor properties like long-term stability, self-calibration and selectivity is discussed. To measure the velocity and direction of wind, three PTC elements are placed under a known angle to each other around a cylindrical flow body. Based on sensor models obtained by pre-operation measurements, the interesting properties are calculated from output voltages by an optimization procedure. Besides the measurement result itself, also its quality follows directly from the optimization output giving a tool to monitor on-line the sensor's state. By periodically changing the power supply of the sensing element and measuring parameters of the resulting thermal impedance, various sources of influence like ambient temperature, rain drops or snow on the device's surface can be separated. Prototype sensors have been developed and evaluated with satisfactory results.

Keywords – environment monitoring, model-based self-monitoring, thermal impedance, smart sensor

I. INTRODUCTION

For consumer market applications, simplicity (costs) and lifetime are generally higher valued than absolute accuracy. It is desired, that during their lifetime the devices work properly without maintenance. The validity of sensor output data in accordance to the specification should be monitored with built-in "smart" monitoring features.

In order to gain the desired information or to improve reliability and selectivity of a sensor, efforts in different 'domains' are taken [1,2].

The inherent so-called 'multi-signal' evaluation refers to all signal processing means applied to extract properties of the measurand in various domains: information is gained from multi-sensors, from different properties of the measured signal in the time/frequency domain, from different locations in space towards an object, from altering between different working points on the sensor's characteristic or from different quantity-related features of the sensor output signal. As a rule, new information is gained by a multiplication of approaches from 'single components' (tools) to 'multi-components'. The entirety of sensor elements and signal processing tools, combined in a smart sensor, can be coined 'multi-component sensors' as an extension of the term 'multi-sensor system' [3]. The question is, what properties have to be extracted and what features are to be determined in order to gain the desired information.

Two sensors, (1) a smart wind sensor composed of merely three PTC (positive temperature coefficient) elements and (2) a simple weather sensor using nothing more than a common temperature-depending Pt100 resistor as the sensing element are described to show what can be gained from some of the multiplication effects in different 'domains' of model-based signal evaluation.

II. THERMAL RESISTANCE EVALUATION

Sensors monitoring the properties of the surrounding medium, in particular wind and weather sensors, are needed for a large variety of everyday applications, including metrology, aviation, transport safety and wind power industry. Conventionally, a cup anemometer and a wind vane are used to measure the wind velocity and the wind direction in horizontal plane, resp. However, due to the mechanical working principle, these systems are often unresponsive in light winds (< 0.5..1 m/s) or when covered by ice or snow. Also, micromachined hot film anemometers working as thermal field variation sensors are being used [4,5]. Measuring the orthogonal temperature gradients with e.g. 4 symmetrical thermopiles, efforts are to be made to compensate for an asymmetric disc heating [6]. Highly reliable sonic anemometers (e.g. [7]) determine the wind speed and direction from transit times of ultrasonic pulses between (mostly three) pairs of transducers. Accurate measurements are available in all weather conditions, but the device is costly.

Sufficient information about the environmental conditions can be gained by observing certain features of temperature-sensitive resistors, positive temperature coefficient (PTC) elements and platinum Pt100 resistors in this case. These sensing elements are available in many different types at very low cost.

For the resistivity of PTC elements, the following model of the temperature-dependent resistance $R_T(T)$ is applied:

$$R_{PTC}(T) = R_{T0} e^{b\left(\frac{T-T_C}{T}\right)} + R_0 \quad (1)$$

where T – sensor temperature, T_C – Curie temperature ($T_C = 373$ K). For most cases, $R_0 = 0$ can be assumed.

At the working point of the $I(U)$ -characteristics, the temperature T of the self-heated sensor element results from the steady state (equilibrium) between the electrical power P_{el}

$$P_{el} = \frac{U^2}{R_{PTC}(T)} \quad (2)$$

and the thermal power P_{th} delivered from the sensor to the environment:

$$P_{th} = \frac{T - T_E}{R_{th}} \quad (3)$$

T_E the temperature of the environment and R_{th} the thermal resistance. As a result, the sensor characteristics is dependent of the temperature of the surrounding medium and the thermal resistance, i.e. its nature and velocity [8,9]. In Fig. 1, measured $I(U)$ -characteristics for different temperatures of the surrounding medium are shown. The simple measurement circuit is shown in Fig. 4.

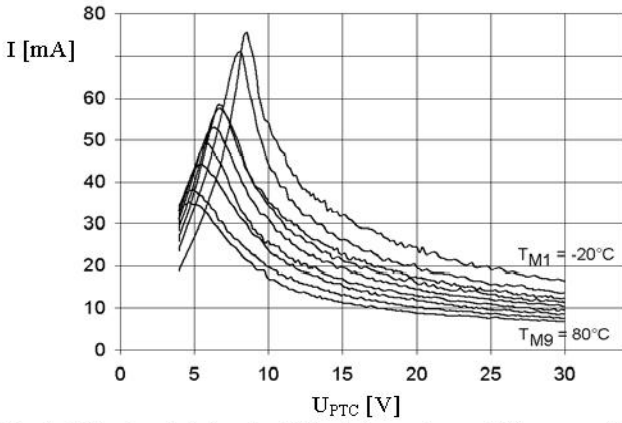


Fig. 1: $I(U)$ characteristics for different temperatures of the surrounding medium

In Fig. 2, measurement data for a voltage range are shown for different environments (air, water) and two different temperatures. Due to the smaller thermal resistance towards liquids, the equilibrium temperature T at the sensor surface and hence the electrical resistivity is lower than for air. For the thermal resistances, $R_{th} \approx 350 \text{ K/W}$ for air and $R_{th} \approx 150 \text{ K/W}$ for water can be assumed, both for room temperature.

For the determination of the unknown model parameters R_{T0} , b and R_{th} , a quality function QF_1 following directly from (1)-(3) is defined:

$$QF_1(R_{T0}, b, R_{th}) = \sum_i \left(\frac{U_i}{R_{T0} \exp\left(b \left(1 - \frac{T_C}{U_i \cdot l_i \cdot R_{th} + T_E}\right)\right)} - I_i \right)^2 \quad (4)$$

As the result of a MSE parameter estimation procedure, calculated for a larger number i of measurements, as an example $R_{T0}=16.6 \text{ } \Omega$, $b=185.93$, $R_{th}=303.6 \text{ K/W}$ are obtained. The fitted data are shown in Fig. 3.

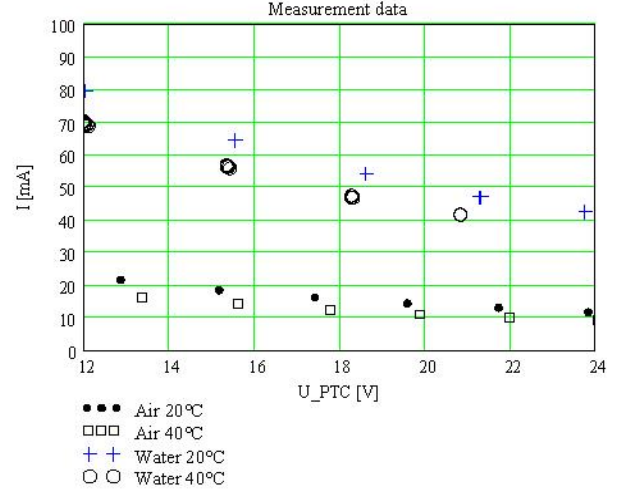


Fig. 2. Measurement data for different environments (air, water) and two different temperatures.

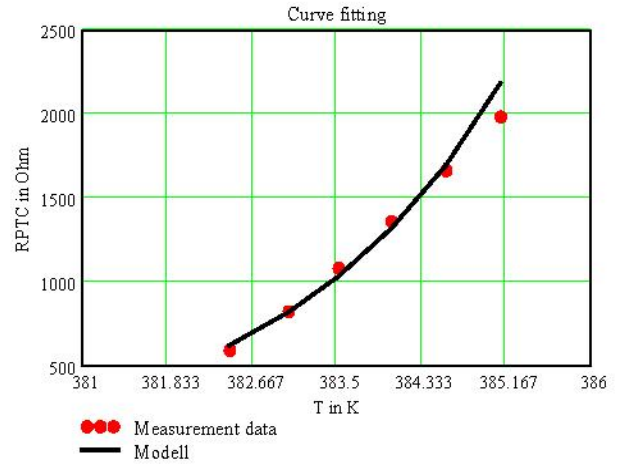


Fig. 3. Result of model parameter estimation and curve fitting

III. MULTI-ELEMENT WIND SENSOR

For wind vector determination, a configuration of three identical PTC elements (Epcos D1010 level sensor in a steel case, length 20 mm, diameter 2 mm), placed under a known angle to each other around a cylindrical flow body, has been examined, see Fig. 1. Because any sophisticated or moving parts can be avoided, the sensor design is very simple and robust. Due to the asymmetrical flow field caused by the construction, the wind velocity v as well as the wind direction α are calculable from simultaneously measured voltages U_k ($k=1,2,3$) from all sensing elements. At the sensing element k voltage is measured which can be modeled as:

$$U_k(v, \alpha, T) = U_{0k}(v, T) + U_{1k} \cdot f(\alpha + \Delta\alpha_k) \quad (5)$$

Here, $\Delta\alpha_1 = 0, \Delta\alpha_2 = 120^\circ, \Delta\alpha_3 = 240^\circ$.

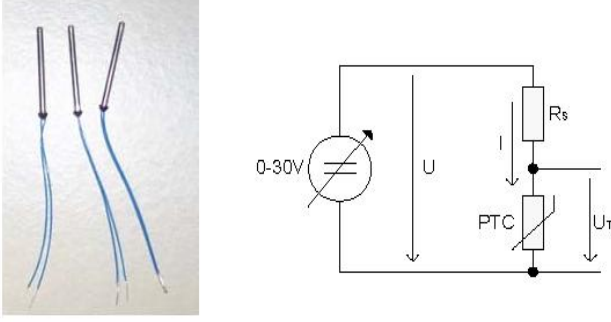


Fig. 4. PTC elements (left) placed under a known angle to each other around a cylindrical solid body (right)

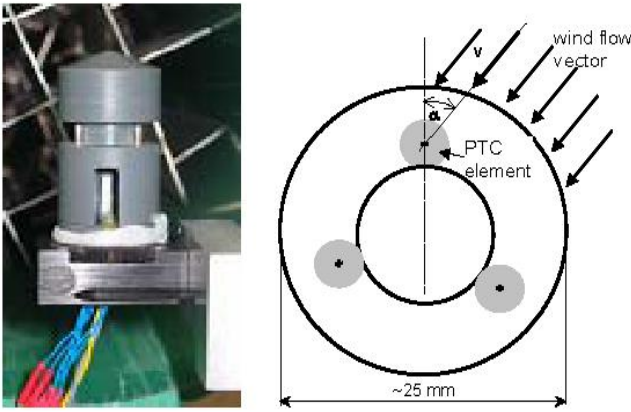


Fig. 5: Wind sensor with three PTC elements (left) placed under a known angle to each other around a cylindrical solid body (right) (A Pt100 resistor for additional temperature measurement is seen in the body. It can be substituted later by appropriate processing of the three voltage readings).

For the estimation of the wind velocity and direction from the actual measurements, an optimization procedure is used. First, the appropriate search region of the optimization produce is found. It is the range of angles for which all 3 output voltages do not change signs with respect to their mean value. The algorithm then starts with an initial guess V of the velocity v from the voltage with the smallest deviation from the mean value of all sensor outputs and its corresponding wind direction A as the initial guess for the angle α . In order to evaluate the sensor performance, a quality function QF_2 is introduced which can be viewed as a geometrical deviation between the estimated point in the (v, α) -plane and the real measurements of all three sensors:

$$QF_2(v, \alpha) = \sqrt{\frac{k \cdot \sum_k (U_k(v, \alpha) - U_k(V, A))^2}{\sum_k U_k(V, A)}} \quad (6)$$

and evaluated for different guesses of V and A . Estimates are accepted or dismissed by threshold decision taking into considering the measurement noise and model error. Hence,

from the optimization output follows directly not only the measurement result itself, but also its quality.

In Fig. 6, the basic principle of the algorithms is shown which is based on finding the minimum deviation (crossing) of two sensor readings in the (v, α) -plane. The optimization produce starts from the right angle with the smallest deviation from the mean value of all sensor outputs. Then, in order to evaluate the sensor performance, a quality function is introduced. Estimates are accepted or dismissed by threshold decision taking into considering the measurement noise and model error. That is, from the optimization output follows directly not only the measurement result itself, but also its quality! In Fig. 7, the value of the “geometrical deviation” between the estimated point in the (v, α) -plane and the real measurements is shown for a certain example. $QF(v, \alpha)$ is drawn in logarithmic scale with v as parameter ($v = 0.5, 0.7, 0.9, 1.0, 1.1, 1.3, 1.5 \text{ m/s}$) in logarithmic scale. The bold line indicates the best fit, resulting in $\alpha = 50^\circ$ and $v = 1 \text{ m/s}$. In Fig. 8, different estimation results are given.

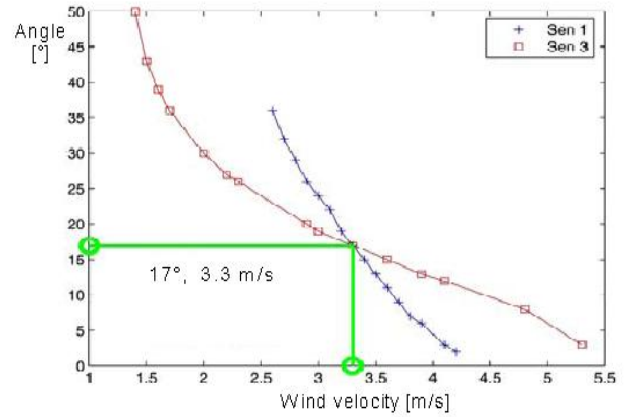


Fig. 6. Finding the minimum deviation of two sensor readings in the (v, α) -plane which defines the wind vector

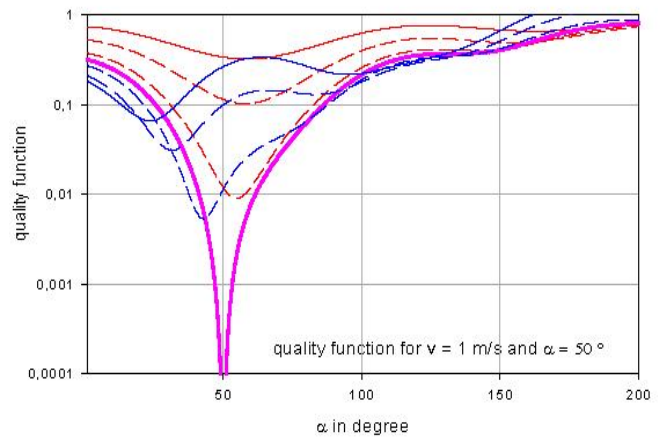


Fig. 7. Figure-of-merit: “Geometrical derivation” between the estimated point in the (v, α) -plane and the real measurements of all three sensors as a function of wind velocity and direction [10]

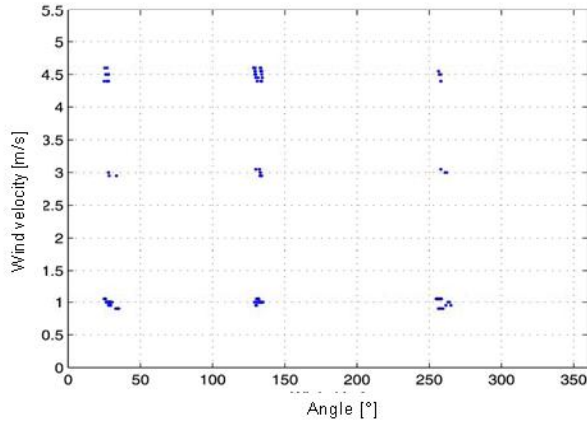


Fig. 8. Estimation of wind velocity and direction: results of the optimization procedure. Given set of conditions: wind velocities 1m/s, 3 m/s, 4.5 m/s, wind directions 30°,140°, 260°.

The accuracies of wind velocity and direction estimation are below 5% and 2°, resp. This is by far sufficient for most applications. In Fig. 9, a comparison of the results of the optimization procedure with the sensor outputs of a state-of-the-art commercial ultrasonic wind sensor (Vaisala WTX50 [7]) are shown.

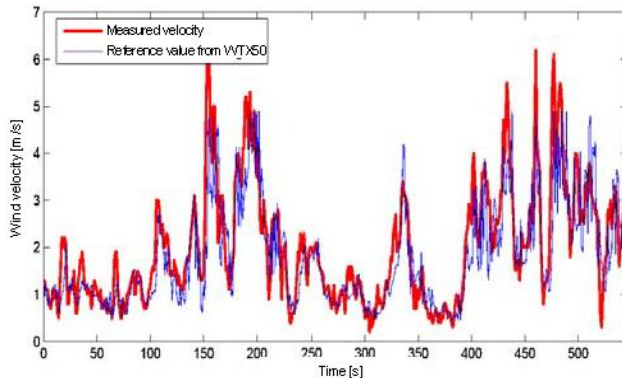


Fig. 9. Comparison of the results of the optimization procedure with the sensor outputs of a reference sensor

Following the ‘domain’ character of signal evaluation, some more information can be gained. For example, an additional temperature sensor normally required for the compensation of the influence of temperature on the sensor output (see Fig. 5) can be substituted by an appropriate processing of the three voltage readings. Also, the increasing influence of dust on the sensor surface changes the sensor characteristic and should be detected and compensated for. This is done during operation by determination of variable parameters of the sensor’s model in appropriate time instants by altering between the working points on the sensor’s I-U characteristics [8].

Furthermore, the optimization algorithm could be accelerated by observing the changes in time of the sensor readings, imposing a upper frequency for possible changes or

using the last finding as a starting point for the next search implying a certain correlation in time between the measurements.

IV. SINGLE-ELEMENT WEATHER SENSOR

The thermal impedance of a self-heating probe gives information about the inside structure, the temperature distribution and the environment conditions in which the probe works [11]. In case of large temperature dependencies of the resistor, sufficiently high periodic power supply with $U_s(t) = U_0 + A \cdot \sin(2\pi f \cdot t + \varphi_U)$ causes a delayed heating of the resistor and, with $I(t) = I_0 + B \cdot \sin(2\pi f \cdot t + \varphi_I)$, results in a periodic change of its resistivity ((I,U)-ellipse), see Fig. 10. The evaluation of specific parameters of the measured (I,U)-ellipse like mean value I_{mean} , phase shift φ , expansion ΔI delivers explicit information about the wind velocity and the presence of rain or snow and ice and as well as about the surrounding temperature. This information is e.g. sufficient to trigger an impulse to an automatically opened window to be closed in case of strong wind or heavy rain fall.

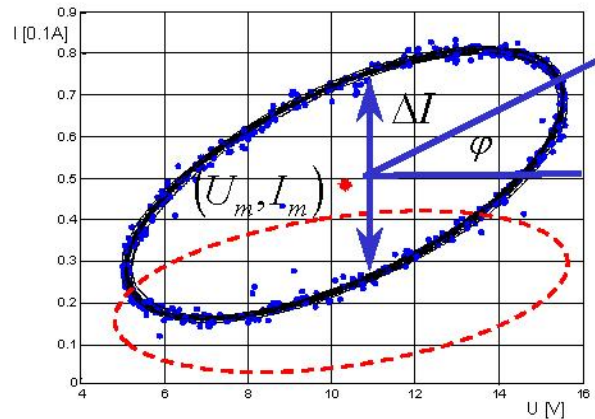


Fig. 10. I-U-characteristics for periodic excitation of Pt100 elements with its main parameters

As a sensor, a platinum Pt100 resistor covered with a larger absorbent foam layer is used. In this case, the sensitive area has a ~20mm diameter, whereas the resistor underneath has an area of about 4 mm². The whole sensor is declined such that rain drops can drain off, Fig. 11.

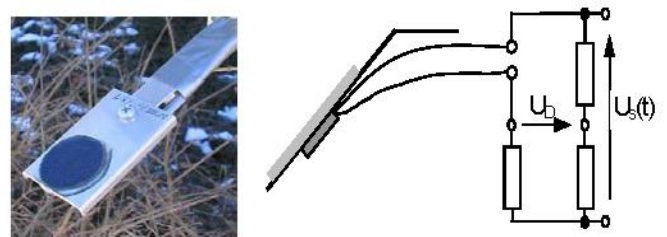


Fig. 11. Weather sensor: View with the resistor attached underneath a water absorbent foam surface (left) and driven in an ohmic bridge arrangement (right)

V. RESULTS

In Fig. 12, I-U characteristics measured for different properties of the surrounding medium (still air wind, rain drops, rain) are shown. It appears, that the mean value (DC part) is largely dependent on the ambient temperature, whereas the magnitude and phase shift (AC part) are dependent on the influences of wind or rain drops. In Fig. 13, the behaviour of the observed parameters as a function of time is demonstrated exemplarily for the mean value of the current for several situations showing the large sensitivity.

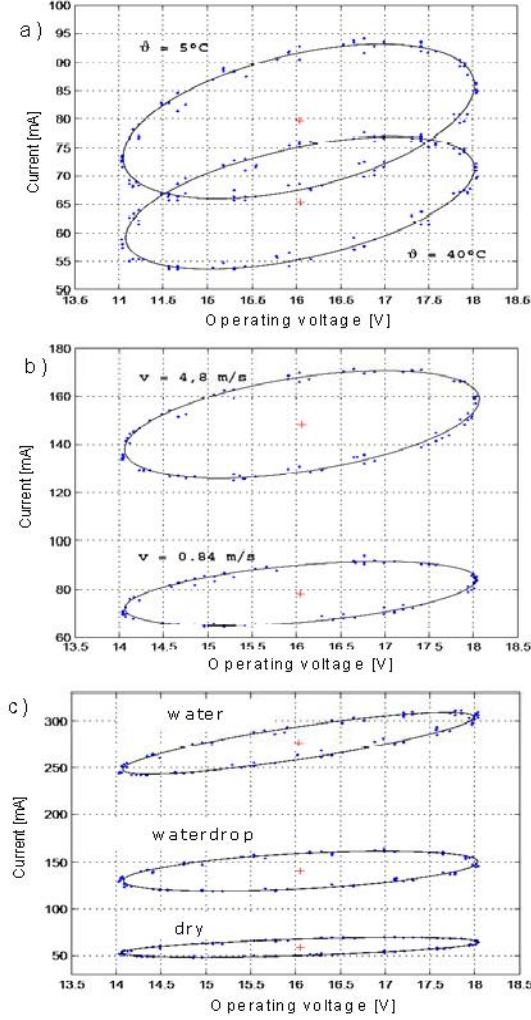


Fig. 12. Measured thermal impedance of a Pt100 resistor influenced by temperature (a), wind velocity (b) and humidity (c)

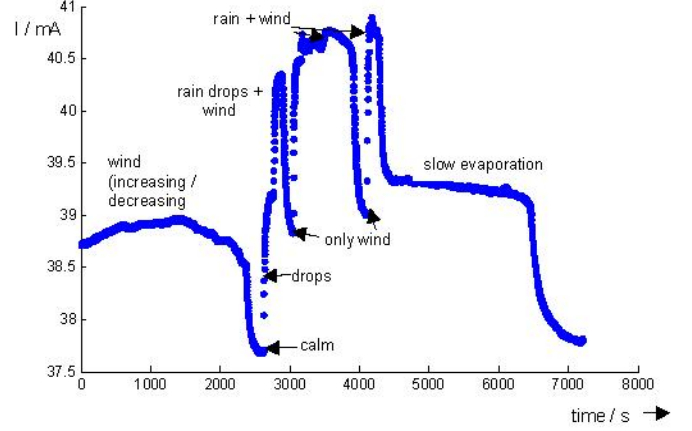


Fig. 13. Behaviour of the mean value as a function of time for different situations



Fig. 14. View of the weather sensor consisting of a simple Pt100-resistor attached below a water absorbent foam surface (above) and general view of the sensor arrangement with reference sensor (Vaisala WTX50)

Using the temperature-depending resistor characteristics $R_T = R_{T0}(1 + \alpha\Delta T)$ and a periodic power supply $U_s = U_{s1} \sin \omega t + U_{s0}$ as well as the approach $T = T_E + |Z_w| \cdot P$ [11], with heat capacity P , $P = P_1 \cdot \sin(\omega t + \varphi_p) + P_0$, the temperature can be modeled as

$$T = T_E + R_{t0}P_0 + R_{t1}P_1 \sin(\omega t + \varphi_T) \quad (7)$$

with the unknown medium temperature T_E , the (unknown) thermal resistivities R_{t0} , R_{t1} and the phase shift φ_T . R_{t0} , R_{t1} depend of the property M of the medium (wind, rain) and the flow velocity v :

$$\begin{aligned} R_{v_0} &= R_{v_0}(v, M) \\ R_{v_1} &= R_{v_1}(v, M) \end{aligned} \quad (8)$$

Hence, these features together with T_E deliver the interesting information leading to the distinction between different weather states. With

$$R_T = R_{T_0} + \alpha R_{T_0} (T_E + R_{v_0} P_0 + R_{v_1} P_1 \sin(\omega t + \varphi_T)) \quad (9)$$

the measured voltage U can be described as

$$U(t) = \frac{U_{s1} \sin \omega t + U_{s0}}{1 + K \cdot (T_E + R_{v_0} P_0) + K \cdot R_{v_1} P_1 \sin(\omega t + \varphi_T)} \quad (10)$$

$$\text{with } K = \frac{\alpha R_{T_0}}{R + R_{T_0}}.$$

From (10), the unknown parameters are determined from the quality function of the least-mean square error.

In Fig. 15, the values of the mean value I_{mean} and phase shift φ from measured I-U-characteristics are compared showing the ability to distinct between different states of the environment.

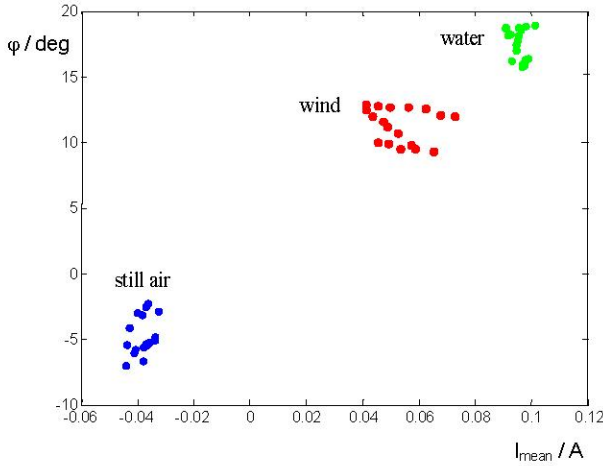


Fig. 15. Result of classification: Parameters for changing thermal impedances of the sensor due to wind and rain drops on its surface

VI. CONCLUSIONS

In many practical applications, low-cost, tiny, remote, maintenance-free and autonomous sensors are increasingly desired. In the paper, the general approach of so called 'multi-component sensors' [3] emphasizing the usage of model-based signal processing tools and particularly built-in monitoring functions to track model parameter changes for enhanced information and selectivity to be gained from very simple and common sensors components has been discussed and exemplarily shown on behalf of simple wind and weather sensors.

In the paper, this abstract and universal principle has been illustrated on behalf of examples using simple temperature-dependent resistors as effective wind and weather sensors.

Among others, an important property of this approach is that the quality of the sensor readings themselves are shown by the optimization output giving a convenient tool to monitor the sensors's state over long-term of operation. Prototype sensors has been deployed and evaluated in real-world conditions, with satisfactory results. The sensor outputs can be further optimized by appropriate choice of the frequencies, AC/DC parts relation and power of the supply voltage. Also, a frequency composition (superposed AC signals) serve to gain information about the sensor's behavior in order to extract the desired information and to monitor the sensor's state.

REFERENCES

- [1] Regtien, P.P.L., Measurement Science for Engineers, Elsevier Butterworth Heinemann, 2004.
- [2] Bentley, J.P., Principles of measurement systems, Longman, London 1983.
- [3] Ruser, H.: Smart weather sensors as an example for 'multi-component' sensors, MFI 2006, IEEE Conf. on Multisensor Fusion and Integration for Intelligent Systems (MFI'06), Heidelberg, 2006
- [4] Mierij Meteo B.V. "Solid State wind sensor MMW005", <http://mierijmeteo.nl>.
- [5] Makinwa K., Huijsing J., A smart wind sensor based on thermal sigma-delta modulation techniques, Sensors & Actuators A97-98: 15-20, 2002.
- [6] Matova S.P., Makinwa, K., Huijsing, J.H., Compensation of packaging asymmetry in a 2-D wind sensor, IEEE Sensors Journal, Vol. 3(6): 761-765, 2003.
- [7] e.g. Vaisala WXT 510 Multi-Parameter Weather Transmitter. <http://vaisala.com>.
- [8] Bradshaw P.: „Thermal methods of flow measurements”, Journal of Scientific Instruments (Journal of Physics E) Series 2, Vol. 1 (1968), pp. 504-509.
- [9] Horn M., Ruser H., Umar L., Self-calibrated PTC air-flow sensor, IEEE Sensors Conf., Orlando, 2002.
- [10] Ruser H., Horn M.: "Smart robust wind sensor using a simple optimization procedure, IEEE Sensors Conf., Irvine, 2005.
- [11] Incropera F.P., DeWitt D.P. Fundamentals of heat and mass transfer, 3rd ed., Wiley, New York 1990.